Research Article

Omer Kalaf, Tauqir Nasir, Mohammed Asmael, Babak Safaei*, Qasim Zeeshan, Amir Motallebzadeh, and Ghulam Hussain

Friction stir spot welding of AA5052 with additional carbon fiber-reinforced polymer composite interlayer

https://doi.org/10.1515/ntrev-2021-0017
received March 20, 2021; accepted March 26, 2021

Abstract: In this study, similar aluminum alloys AA5052 with additional carbon fiber-reinforced polymer composite (CFRP) interlayer were selected to investigate the effect of welding parameters (rotational speed and dwell time) on the mechanical properties, joint efficiency, and microstructure of friction stir spot weld joint. The maximum tensile shear load was 1779.6 N with joint efficiency of 14.6% obtained at rotational speed of 2,000 rpm and 2 s dwell time, which is 39.5% higher than the value at low rotational speed 850 rpm and 2 s dwell time. Meanwhile, the maximum microhardness 58 HV was attained in the keyhole region at rotational speed of 2,000 rpm and dwell time of 5 s, which is 22.4% higher compared to low rotational speed. The SEM-EDS results reveal the presence of intermetallic compounds (Al–Mg–C), which enhance the intermetallic bonding between elements.

Keywords: friction stir spot welding, interlayer, carbon fiber-reinforced polymer composite, aluminum alloys, mechanical properties, microstructure

1 Introduction

There is an increasing demand for lightweight structures, especially in transportation sector [1]. Recently, applications of lightweight materials such as aluminum, magnesium, and metal foams, as typical porous materials [2], have been increased in automotive and aerospace industries [3]. Also, it is a critical challenge to reduce the weight in these industries to improve the performance of vehicle and airplane [4]. Light weight structure designs can be achieved by using composite materials, which are high cost-intensive and yet not suitable for mass production due to the necessity of manual processing [5]. In recent years, composite materials have triggered worldwide investigations to manufacture improved structures with superior mechanical characteristics [6] same as laminated composite plates [7]. Carbon fiber-reinforced composites (CFRPs) have excellent thermal and mechanical properties and are commonly applied in the fabrication of polymer–matrix composites [8]. Composite and nanocomposite materials are utilized as a lightweight material [9]. CFRP industry is developing by constant growth of demand from defense and aerospace to automotive sectors [10]. In the past decades, nanocomposite and composite materials have attracted great attention because of their exclusive improving and properties' effects on specific mechanical performance which are not easy to achieve with other materials [11]. New micro- and nano-technologies used in fabrication of advanced materials have been resulted in lightweight structures with a large range of applications [12]. Despite the fact that the extraordinary mechanical characteristics of CFRPs make them an attractive option for designers, they have to outperform existing lightweight structural automotive materials [13], whereas carbon nanotubes are suitable for electrical and thermal application [14]. Moreover, reinforcing core layer with CNTs leads to remarkable drop and increase in thermal and mechanical buckling resistances,

* **Corresponding author: Babak Safaei,** Department of Mechanical Engineering, Eastern Mediterranean University, Famagusta, North Cyprus via Mersin 10, Turkey, e-mail: babak.safaei@emu.edu.tr
Omer Kalaf, Tauqir Nasir, Mohammed Asmael, Qasim Zeeshan: Department of Mechanical Engineering, Eastern Mediterranean University, Famagusta, North Cyprus via Mersin 10, Turkey
Amir Motallebzadeh: Koç University Surface Science and Technology Center (KUYTAM), Sariyer, Istanbul, Turkey
Ghulam Hussain: Faculty of Mechanical Engineering, GIK Institute of Engineering Sciences and Technology, Topi, 23460, Pakistan

Open Access. © 2021 Omer Kalaf *et al.*, published by De Gruyter. This work is licensed under the Creative Commons Attribution 4.0 International License.

respectively [15]. Rezaei *et al.* [16] proposed the effect of fiber length on thermomechanical properties of carbon fiber. The results show that short carbon fiber-reinforced polypropylene thermal stability increased by increasing the length of carbon fiber. Therefore, extensive research has been performed on the application of conventional pitch-based CFRPs in improving and optimizing the characteristics of a wide variety of structures [17]. The machining of CFRP composites types is carried out mainly on plain-woven carbon fiber and epoxy resin matrix, including directional, unidirectional, and multidirectional CFRP laminates [18]. Aluminum alloys are one of the most promising lightweight materials due to their corrosion resistance, high specific stiffness, strength, high recyclability, and impact resistance [19]. Friction stir spot welding FSSW is a solid state joining technique and has been applied to aluminum alloys such as 2,000 and 5,000 series [20]. These alloys are apt to solidification and liquation cracking, which can be avoided by friction stir spot welding [21]. FSSW is an advanced form of friction welding which is mostly used to weld the similar and dissimilar alloys [22]. FSSW provides reduction in energy consumption up to 90 and 40% in capital cost compared to resistance spot welding (RSW) [23]. Also, the formation of stirring zone in FSSW requires a small amount of heat generation which reduces welding time and energy consumption [24]. Procesov [25] showed the comparison between FSSW and RSW of AA5005 alloy. The results showed that the mechanical performance of FSSW joint was higher than RSW and concluded that FSSW could be an alternative to RSW. The most important parameter for heat input in friction stir spot welding is rotational speed [26] and peak temperature increased with increased rotational speed [27]. The temperature should be less than melting point of metals during the processes [28]. Rana *et al.* [29] presented the effect of different rotational speed on FSSW; the optimal rotational speed was 1,800 rpm for high mechanical performance. High rotation speed causes high temperature, and as a result, more intensive stirring and mixing of the material and that energy was positively connected to the bonding area with long weld strength [30]. Due to fixed pin length and shoulder, only a single lap joint could be welded with constant thickness during friction stir spot welding [31]. Dwell time is another parameter affecting FSSW and provides the heat required for the formation of stir zone and bonding region between upper and lower sheets [32]. Long dwell times should be applied for metals with high melting points to generate required heat for plasticity flow material [33]. Also, less than one second would be small softening in heat-affected zone for heat-treated aluminum alloys [34]. Rafiei *et al.* [35] investigated the mechanical properties of dissimilar friction welding of aluminum (AA5052)-magnesium and aluminium (AA2024)-copper. The processes parameters were rotational speed 1,250 rpm and feed rate 160 mm/min. The hardness was low in heat-affected zone and thermal-mechanical-affected zone (TMAZ) due to welding defects such as hook defect. Also, residual stress is considered as a defect on welding quality [36]. Khosa *et al.* [37] evaluated the effect of thermomechanical during FSSW of AA6082-T6. The result showed that the effect of temperature on the microstructure and mechanical properties was severe due to the deformation and material flow of welded sample. Kubit *et al.* [38] studied additional sealant interlayer in AA7075-T6 alloy. The obtained results show that the joint properties of weld joint could be improved by optimal thickness of interlayer. Sadoun *et al.* [39] evaluated the effect of interlayer in dissimilar aluminum AA2024 and AA7075 alloys. The obtained result showed 18% improvement in joint strength due to grain refinement compared to without interlayer joint. Andre *et al.* [40] improved the adhesion mechanisms and mechanical performance of aluminum AA2024-T3 and CFRP with 100 μm PPS film additional interlayer fiction spot welding. The effect of micro-mechanical interlocking at the interface of interlayer achieved with sandblasted specimens was clear. The optimal tensile shear force was 3,068 N, due to effect on contact surface area. Also, sandblasting was found to be the most effective treatment which maximized joint mechanical performance. Andre *et al.* [41] investigated the effects of rotating speed and joining pressure on the mechanical strength and microstructure of friction spot welding of carbon fiber and aluminum AA2024-T3 with 100 μm PPS film interlayer. They reported that lap shear force was increased from 2,700 to 3,070 N, which was higher than those for joints without interlayer because of their improved micro-mechanical interlocking, better load distribution, and larger bonding area. Temperature was measured on surface which ranged from 325 to 417°C. In the microstructure of two bonding interfaces, the PPS into the crevices of aluminum and CFRP entrapment by aluminum deformed. However, in joints without interlayer, a transition zone with high air bubbles was created between adhesion zone and plastically deformed zone. Abed *et al.* [42] proposed the effect of friction stir spot welding of AA6061-T6 with copper interlayer and found that the increase of dwell time and plunge depth was beneficial to the formation of joint and directly increased tensile shear load. Joint formation was improved with cupper interlayer addition and this improvement could be related to the increase of bonding area and

intermetallic compound from the reaction of metal and interlayer. High load fracture occurred in cupper interlayer rather than those without interlayer. However, interlayer considerably increases the protection of weld against corrosive environments [43]. The reaction between aluminum and carbon fiber during welding processes caused to form aluminum carbide (Al_4C_3) at temperatures above 500°C, which negatively affected the performance of interfacial layer in composites [44].

In the current study, the effect of welding parameters and CFRP interlayer on the mechanical and microstructural properties of welding joints has been investigated in FSSW joint process. The objective of this study is to evaluate the effect of CFRP interlayer on the performance of mechanical properties (tensile shear load and microhardness) and microstructural properties (SEM-EDS) and joint efficiency of the weld joints.

2 Experimental work

Aluminum alloy AA5052 plates were chosen in this study. The dimensions of the plate were 100 mm × 25 mm × 4 mm, based on American Welding Society standard (AWS C1.1M/C1.1:2012) [42] as showed in Figure 1(a). CFRP with thickness 0.5 mm was applied as interlayer between similar aluminum sheets. For each combination of process parameters, three replicates were made. The surface of material was cleaned using alcohol to remove contaminants that could generate oxides. The tool was rotated at high speed, then forced into workpiece until the shoulder contacted top metal surface.

The tool was made from steel alloy AISI 4340 (UNS G43400), as showed in Figure 1b. The length of the pin was 6.2 mm and its diameter was 5 mm with cylindrical design. Friction stir spot welding consists of three stages: plunging, stirring, and retracting, as showed in Figure 2.

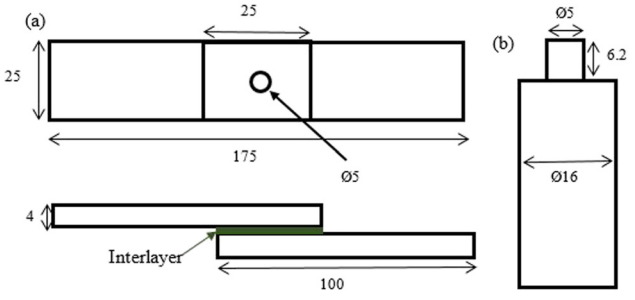

Figure 1: (a) Schematic diagram of lab joint (mm); (b) tool dimension (mm).

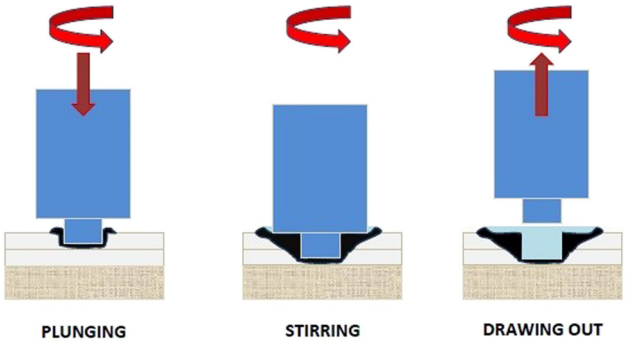

Figure 2: Friction stir spot welding processes.

The experimental full factorial design with two level (rotation speed and dwell time) was chosen for joining processes, as illustrated in Table 1.

In this study, temperature evolution on the top surfaces of aluminum was monitored during friction stir spot welding (Thermometer PCE-T390). The maximum process temperature was considered as the highest temperature measured on the top surfaces of aluminum sheets. The mechanical performance of joints was evaluated through tensile shear load by using universal tensile test machine (INSTRON-5582). Three identical samples were tested for each joining condition. Load rate was adjusted at 3 mm/min for all specimens and were mounted on the jaws of the machine. Joint efficiency (η) of AA5052 with CFRP was obtained by applying the following equation [45].

$$\text{Efficiency } (\eta) = \frac{\text{Tensile shear load of weld joint}}{\text{Tensile shear load base metal}} \times 100\% \quad (1)$$

Microhardness values were evaluated using Vickers test with Vickers hardness of 4.903 N and dwell time 20 s. Several indents were made at 10 mm intervals along cross section from weld center to investigate microhardness profile. Microstructure analysis was conducted in the

Table 1: Two-level 2^k full factorial design: experiments defined by normalized parameters (rotation speed and dwell time)

Sample no.	Std order	Run order	Rotational speed	Dwell time (s)
1	2	1	850	5
2	5	2	200	2
3	1	3	850	2
4	4	4	1,300	5
5	6	5	2,000	5
6	3	6	1,300	2

cross section of the joint by optical microscope. Also, in microstructure evaluation, energy dispersive spectroscopy (SEM-EDS) was applied.

3 Results and discussions

3.1 Temperature evaluation

Figure 3 shows peak temperature of aluminum and CFRP interlayer at different rotational speed and dwell time. The peak temperature was about 298.5°C at rotational speed 2,000 rpm and dwell time 5 s, while the minimum temperature was 216.9°C at rotational speed 850 rpm and dwell time 2 s. Generally, Al_4C_3 compound could not be formed due to low temperature during the FSSW processes. Also, it was clear that the increase of dwell time from 2 to 5 s at all rotating speeds directly affected temperature, dramatically increasing it by up to 10%. Heat generation at the surface of aluminum was not high enough to melt the interlayer at the interface in the whole overlapped area. This was due to the lower thermal conductivity of CFRP (0.19 W/m K) than aluminum [46].

3.2 Tensile shear load

The results of tensile shear load of AA5052 FSSW joints are showed in Figure 4. Maximum tensile of 1779.6 N was produced at rotational speed 2,000 rpm and dwell time 2 s with 14.6% joint efficiency, while minimum tensile occurred at 850 rpm and dwell time 2 s was 1,373 N. In addition, the results showed that increase of rotational speed from 850 to 2,000 rpm at 2 s dwell time with 39.5% improvement in tensile shear load was obtained. It was

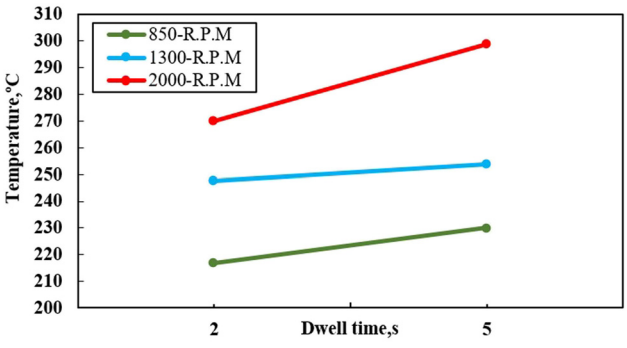

Figure 3: Evolution of friction spot joining process temperature.

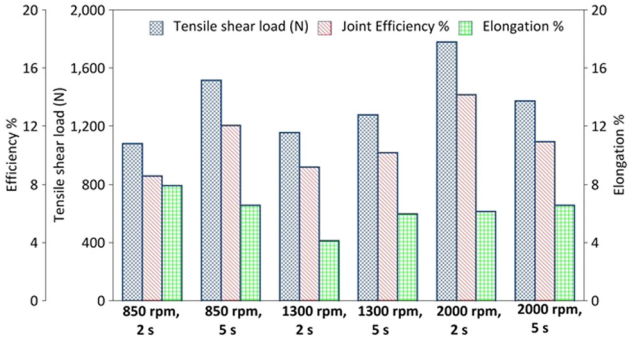

Figure 4: Tensile shear load (N), elongation (%), and efficiency (%) of FSSW.

necessary to decrease the distribution of intermetallic compounds to have high tensile and avoid poor performance of welding [45]. The highest tensile shear load could be related to the large bonding area and good load distribution in FSSW process [47]. On the other hand, increase of dwell time from 2 to 5 s and a 9% decline in tensile shear load at low to high rotational speeds caused to increase heat input that led to overheat the material in weld region, which induced the grain growth and eventually decreased tensile shear load [41,48]. High heat input was developed due to high dwell time, which led to initiate the cracks in the weld interface and reduce the tensile shear load [49]. The maximum elongation of 8% was founded at rotational speed of 850 rpm and 2 s of dwell time. Large elongation could be due to large joint area and increased amount of CFRP attached to aluminum surface [50].

3.3 Microhardness

Rotational speed and dwell time are significant parameters in FSSW processes, such that increase of dwell time from 2 to 5 s at all rotational speeds directly increased microhardness. Microhardness profile is illustrated in Figure 5. Maximum microhardness value was 58 HV which was obtained at 2,000 rpm rotating speed and 5 s dwell time in keyhole, whereas minimum value was 24.5 HV obtained at 1,300 rpm rotational speed and 2 s dwell time in stir zone (SZ). The graph showed the highest microhardness in keyhole area rather than SZ and TMAZ. In key hole area, 29% improvement was achieved by increasing rotational speed and dwell time. This was due to mixing and incorporating CFRP and aluminum during FSSW processes. Hardness test results provided further support to the fact that large amounts of CFRP were uniformly dispersed in the matrix over large

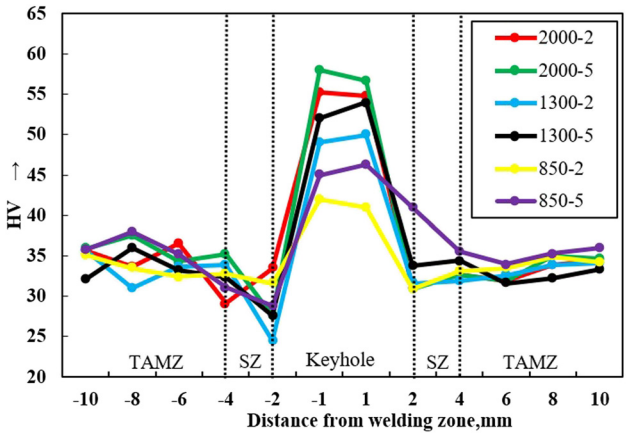

Figure 5: Microhardness distributions of welds at different rotational speed and dwell time.

region. However, heat generation during FSSW minimized microhardness in TMAZ region. Large amounts of geometrically necessary dislocations (GNDs) [51,52] induced during FSSW are thought to be an important reason of strengthening. There was a large difference in the coefficient of thermal expansion (CTE) between AA5052 (23.8X10-6 K-1) and CFRP (5.5X10-6 K-1) along transverse and longitudinal directions, respectively. The mismatch of CTE led to the generation of GNDs during FSSW [44]. Hence, hardness in SZ and TMAZ could be attributed to the comprehensive effect of variations in grain size and strengthening of precipitates [53].

3.4 Microstructure

The microstructure of AA5052 with CFRP interlayer was presented in this study. Weld microstructure depended on the type of the process applied, welding parameters, and workpiece material properties such as thermal conductivity and external cooling conditions [49]. Nub was slightly inserted into thermoplastic composite part, which consequently increased mechanical interlocking between joining partners and contributed to joint mechanical strength under shear loading [54]. The samples of rotational speed 850 rpm and dwell times 2 and 5 s had lower mechanical performance compared with those at 2,000 rpm. The main reason for this was low

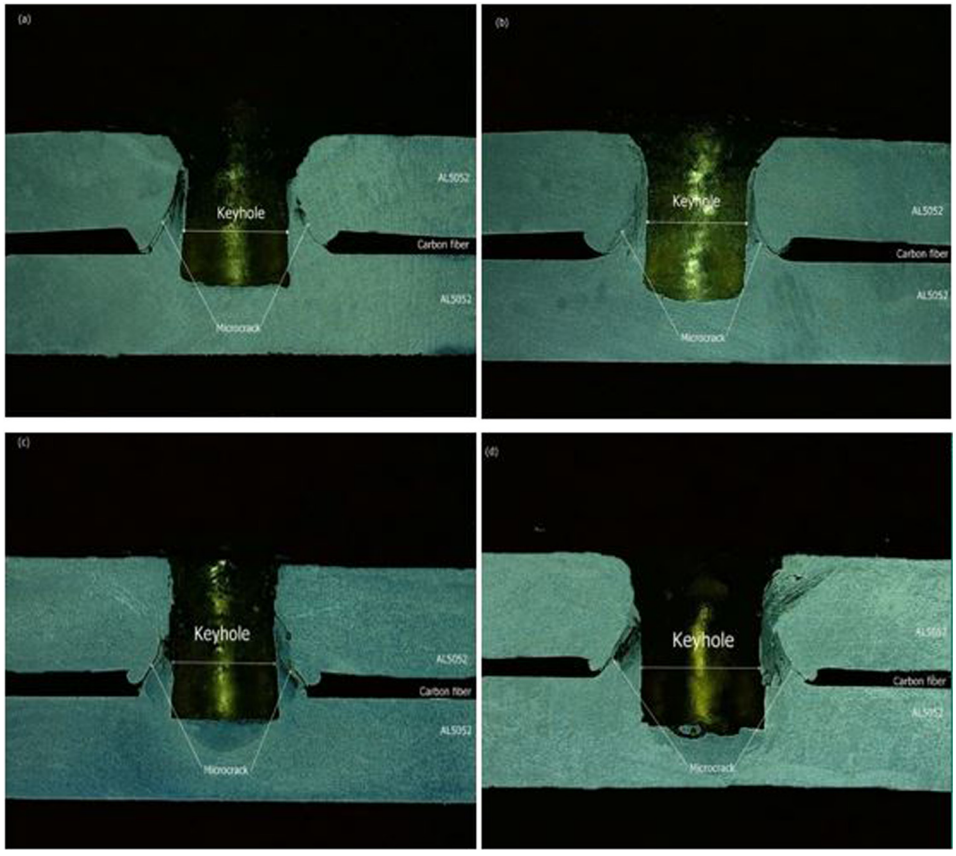

Figure 6: Cross section of the welding of samples (a) 850 rpm and 2 s. (b) 850 rpm and 5 s. (c) 1,300 rpm and 5 s. (d) 2,000 rpm and 2 s.

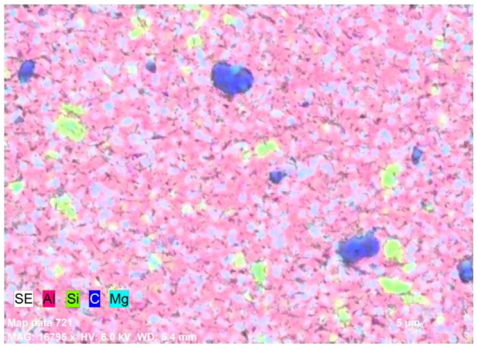

Figure 7: Element distribution of Al and CFRP joint.

heat input during FSSW process, which was not enough to melt interlayer to improve microhardness, as shown in Figure 6(a and b). In the cross section joint of 1,300 rpm and 5 s, crack was observed under tool pin after welding. Cracks on right and left sides rapidly extended along the top surface to pull out the entire joint from the upper plate. In the hook defect, the crack initiation was identified and extended along the hook toward the top surface to pull out stir zone; meanwhile, cracks at hook defect on the left side extended along the hook toward the bottom of stir zone. The joint broke along the interface and only a small part was pulled out. Microcracks in stirring zone were clear and their number was increased by increasing rotational speed and dwell time, as showed in Figure 6(c).

In cross section joint at rotation speed 2,000 rpm and dwell time 2 s, interlayer was melted and squeezed out of the center to the edges of the joint. This was due to high temperatures (about 298.5°C) during welding process which led to the melting of interlayer at the center of the joint. This occurred due to lower molten viscosity associated with higher frictional energy generation in this region [46]. The molten polymer could flow into crevices on aluminum surface during joining process. This caused micro-mechanical interlocking between parts, leading to increased tensile shear load, as showed in Figure 6(d) [55].

According to the microstructural characteristics of grain size and precipitates, it was found that weld structure was symmetrical with respect to tool axis. FSSW produced SZ or nugget and TMAZ, which could be identified in sequence from keyhole periphery towards base

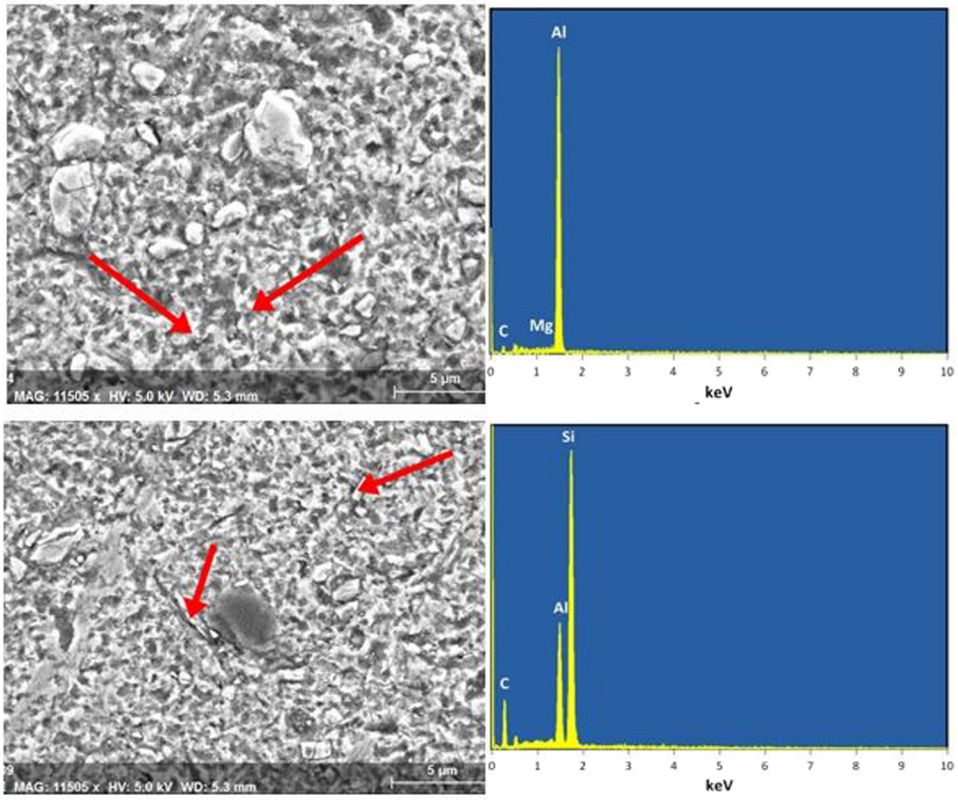

Figure 8: SEM-EDS analyses of friction stir spot welding zone: 2,000 rpm and 2 s dwell time.

material. During tool penetration in friction stir spot welding, rapid strain rates and heating were imposed by rotating tool. In conventional friction stir spot welding method, a stir zone structure containing fine equaled grains fully develops near the end of penetration process when the tool is almost completely penetrated into sheets. Evidence of such cracking was also noted in AA7075 refill friction stir spot welds, as reported by Shen *et al.* [20]. The formation of a shiny surface on friction stir spot welds combination of material and welding parameters may be prone cracking. Plastic deformation and high temperature induced local melting and it was argued that liquation and solidification occurred repeatedly due to oscillating temperature resulting in nonequilibrium solidus temperature. This paper (SEM-EDS) analyzed the welds produced at rotational speed 2,000 rpm and dwell time 2 s. Similar aluminum alloys made strong bonds with CFRP.

It is necessary to uniformly distribute CFRP in the matrix for fabricating aluminum alloys with CFRP and the results showed that the concentration of aluminum and carbon elements confirmed chemical bonding between aluminum and molten CFRP interlayer. Also, SEM-EDS analysis was performed to the compositions, to take place and form intermetallic compound. Dwell time was the main effect parameter to provide time for the diffusion. Figure 7 presents an SEM-EDS mapping microanalysis to identify the chemical intermetallic composition of the phases present in the welding joint and disruptions of carbon particles into the matrix, which might significantly affect structures and their properties.

Moreover, aluminum carbide (Al_4C_3) was not observed because of low heat input during welding processes (Max. 298.5°C). Contact and bonding between CFRP and AA5052 was high due to thermal-mechanical effect.

The presence of Al, Mg, and C elements was proved, as illustrated in Figure 8, which indicated the presence of strong bonding, and there may be mechanical interlocking leading to high adhesive forces at joint areas which was due to the presence of carbon molecular bonding. [56]. Also, Figure 8 shows ternary intermetallic compound (Al–Si–C) and these elements mixed together due to heat input during friction processes between aluminum and CFRP [57,58]. These compounds might increase microhardness by about 58% in keyhole rather than in SZ and TMAZ [59]. In addition, more carbon fiber increased microhardness. On the other hand, more fiber reduced the distance between aluminum and fibers and increased stress, which decreased the strength of composites [60].

4 Conclusions

The current study demonstrated that similar aluminum alloys 5052 with additional CFRP interlayer were successfully joined by applying friction stir spot welding. The effect of tool rotational speed and dwell time on mechanical performance and microstructure was investigated. The following conclusions were drawn:

- The maximum tensile shear load was obtained at rotational speed 2,000 rpm and 2 s dwell time with joint efficiency of 14.61%. The increase of tensile load due to heat input melted CFRP interlayer and squeezed out of the center, whereas low rotational speed had low value of tensile shear load. Consequently, this decrease in tensile shear load may be due to the formation of microcracks within the stir zone.
- The maximum hardness was observed at rotational speed 2,000 rpm and 5 s dwell time, which gradually reduced by decreasing rotational speed and dwell time. The increase in key hole area was due to plastic deformation rather than SZ and TMAZ. Carbon fiber interlayer and welding parameters showed significant effect on microhardness result. This was due to highly different coefficients of thermal expansion, mixing, and incorporating between AA5052 sheets and CFRP interlayer.
- In the microstructural, the main discrete regions observed in FSSW joints are SZ and TMAZ. Interlayer was melted and squeezed out of the center of edge joint due to high heat input during the processes. Scanning electron microscope showed welding defects such as cracks which were clearly observed on the left and right sides of keyhole and were increased by increasing welding parameters. Also, SEM-EDS analysis was applied to observe the intermetallic compound and their element distribution. The elements such as Al, Mg, and C increase the mechanical performance.

Funding information: The authors state no funding involved.

Author contributions: All authors have accepted responsibility for the entire content of this manuscript and approved its submission.

Conflict of interest: The authors state no conflict of interest.

References

[1] Dong H, Tang Z, Li P, Wu B, Hao X, Ma C. Friction stir spot welding of 5052 aluminum alloy to carbon fiber reinforced polyether ether ketone composites. Mater Des. 2021;201:109495.

[2] Gao W, Qin Z, Chu F. Wave propagation in functionally graded porous plates reinforced with graphene platelets. Aerosp Sci Technol. 2020;102:105860.

[3] Lambiase F, Grossi V, Di Ilio A, Paoletti A. Feasibility of friction stir joining of polycarbonate to CFRP with thermosetting matrix. Int J Adv Manuf Technol. 2020;106(5):2451–62.

[4] Cinar Z, Asmael M, Zeeshan Q, Safaei B. Effect of springback on A6061 sheet metal bending: a review. J Kejuruteraan. 2021;33(1):13–26.

[5] Frketic J, Dickens T, Ramakrishnan S. Automated manufacturing and processing of fiber-reinforced polymer (FRP) composites: an additive review of contemporary and modern techniques for advanced materials manufacturing. Addit Manuf. 2017;14:69–86.

[6] Sahmani S, Safaei B. Large-amplitude oscillations of composite conical nanoshells with in-plane heterogeneity including surface stress effect. Appl Math Modell. 2021;89:1792–813.

[7] Safaei B. The effect of embedding a porous core on the free vibration behavior of laminated composite plates. Steel Compos Struct. 2020;35(5):659–70.

[8] Behdinan K, Moradi-Dastjerdi R, Safaei B, Qin Z, Chu F. Hui D. Graphene and CNT impact on heat transfer response of nanocomposite cylinders. Nanotechnol Rev. 2020;9(1):41–52.

[9] Moradi-Dastjerdi R, Behdinan K. Free vibration response of smart sandwich plates with porous CNT-reinforced and piezoelectric layers. Appl Math Modell. 2021;96:66–79.

[10] Heggemann T, Homberg W. Deep drawing of fiber metal laminates for automotive lightweight structures. Compos Struct. 2019;216:53–7.

[11] Fan F, Sahmani S, Safaei B. Isogeometric nonlinear oscillations of nonlocal strain gradient PFGM micro/nano-plates via NURBS-based formulation. Compos Struct. 2021;255:112969.

[12] Fattahi A, Safaei B, Moaddab E. The application of nonlocal elasticity to determine vibrational behavior of FG nanoplates. Steel Compos Struct. 2019;32(2):281–92.

[13] Tripathi K, Vincent F, Castro M, Feller J. Flax fibers–epoxy with embedded nanocomposite sensors to design lightweight smart bio-composites. Nanocomposites. 2016;2(3):125–34.

[14] Talebizadehsardari P, Eyvazian A, Asmael M, Karami B, Shahsavari D, Mahani RB. Static bending analysis of functionally graded polymer composite curved beams reinforced with carbon nanotubes. Thin-Walled Struct. 2020;157:107139.

[15] Moradi-Dastjerdi R, Behdinan K, Safaei B, Qin Z. Buckling behavior of porous CNT-reinforced plates integrated between active piezoelectric layers. Eng Struct. 2020;222:111141.

[16] Rezaei F, Yunus R, Ibrahim N. Effect of fiber length on thermomechanical properties of short carbon fiber reinforced polypropylene composites. Mater Des. 2009;30(2):260–3.

[17] Yu T, Soomro SA, Huang F, Wei W, Wang B, Zhou Z, et al. Naturally or artificially constructed nanocellulose architectures for epoxy composites: a review. Nanotechnol Rev. 2020;9(1):1643–59.

[18] Asmael M, Safaei B, Zeeshan Q, Zargar O, Nuhu AA. Ultrasonic machining of carbon fiber–reinforced plastic composites: a review. Int J Adv Manuf Technol. 2021;113:3079–120.

[19] Lapčík L, Vašina M, Lapčíková B, Hui D, Otyepková E, Greenwood RW, et al. Materials characterization of advanced fillers for composites engineering applications. Nanotechnol Rev. 2019;8(1):503–12.

[20] Shen Z, Ding Y, Gerlich AP. Advances in friction stir spot welding. Crit Rev Solid State Mater Sci. 2020;45(6):457–534.

[21] Ilman MN. Microstructure and mechanical properties of friction stir spot welded AA5052-H112 aluminum alloy. Heliyon. 2021;7(2):e06009.

[22] Nasir T, Asmaela M, Zeeshana Q, Solyalib D. Applications of machine learning to friction stir welding process optimization. J Kejuruteraan. 2020;32(1):171–86.

[23] Feng Z, Santella M, David S, Steel R, Packer S, Pan T, et al. Friction stir spot welding of advanced high-strength steels–a feasibility study. SAE Trans. 2005;114:592–8.

[24] Saunders N, Miles M, Hartman T, Hovanski Y, Hong S-T, Steel R. Joint strength in high speed friction stir spot welded DP 980 steel. Int J Precis Eng Manuf. 2014;15(5):841–8.

[25] Procesov EPO. Experimental comparison of resistance spot welding and friction-stir spot welding processes for the en aw 5005 aluminum alloy. Mater Tehnol. 2011;45(5):395–9.

[26] Su P, Gerlich A, North T, Bendzsak G. Energy generation and stir zone dimensions in friction stir spot welds. SAE Trans. 2006;115:717–25.

[27] Gerlich A, Yamamoto M, North T. Strain rates and grain growth in Al 5754 and Al 6061 friction stir spot welds. Metall Mater Trans A. 2007;38(6):1291–302.

[28] Kumar Rajak D, Pagar DD, Menezes PL, Eyvazian A. Friction-based welding processes: friction welding and friction stir welding. J Adhes Sci Technol. 2020;34(24):2613–37.

[29] Rana PK, Narayanan RG, Kailas SV. Effect of rotational speed on friction stir spot welding of AA5052-H32/HDPE/AA5052-H32 sandwich sheets. J Mater Process Technol. 2018;252:511–23.

[30] Paidar M, Mehrez S, Ojo O, Mohanavel V, Babaei B, Ravichandran M. Modified friction stir clinching of AA6061-T6/AA5754-O joint: effect of tool rotational speed and solution heat treatment on mechanical, microstructure, and fracture behaviors. Mater Charact. 2021;173:110962.

[31] Li M, Zhang C, Wang D, Zhou L, Wellmann D, Tian Y. Friction stir spot welding of aluminum and copper: a review. Materials. 2020;13(1):156.

[32] Paidar M, Ali KA, Mohanavel V, Mehrez S, Ravichandran M, Ojo O. Weldability and mechanical properties of AA5083-H112 aluminum alloy and pure copper dissimilar friction spot extrusion welding-brazing. Vacuum. 2021;187:110080.

[33] Al-Sabur R, Jassim AK, Messele E. Real-time monitoring applied to optimize friction stir spot welding joint for AA1230 Al-alloys. Mater Today Proc. 2021;42:2018–24.

[34] Ahmad R, Asmael M. Effect of aging time on microstructure and mechanical properties of AA6061 friction stir welding joints. Int J Automot Mech Eng. 2015;11:2364.

[35] Rafiei R, Shamanian M, Fathi M, Khodabakhshi F. Dissimilar friction-stir lap-welding of aluminum-magnesium (AA5052) and aluminum-copper (AA2024) alloys: microstructural evolution and mechanical properties. Int J Adv Manuf Technol. 2018;94(9–12):3713–30.

[36] Glaissa MAA, Asmael M, Zeeshan Q. Recent applications of residual stress measurement techniques for FSW joints: A. J Kejuruteraan. 2020;32(3):357–71.
[37] Khosa SU, Weinberger T, Enzinger N. Thermo-mechanical investigations during friction stir spot welding (FSSW) of AA6082-T6. Weld World. 2010;54(5):R134–46.
[38] Kubit A, Wydrzynski D, Trzepiecinski T. Refill friction stir spot welding of 7075-T6 aluminium alloy single-lap joints with polymer sealant interlayer. Compos Struct. 2018;201:389–97.
[39] Sadoun A, Meselhy A, Deabs A. Improved strength and ductility of friction stir tailor-welded blanks of base metal AA2024 reinforced with interlayer strip of AA7075. Results Phys. 2020;16:102911.
[40] Manente André N, Goushegir SM, Scharnagl N, dos Santos JF, Canto LB, Amancio-Filho ST. Composite surface pre-treatments: Improvement on adhesion mechanisms and mechanical performance of metal–composite friction spot joints with additional film interlayer. J Adhes. 2018;94(9):723–42.
[41] André NM, Goushegir SM, Dos Santos JF, Canto LB, Amancio-Filho ST. Friction Spot Joining of aluminum alloy 2024-T3 and carbon-fiber-reinforced poly (phenylene sulfide) laminate with additional PPS film interlayer: Microstructure, mechanical strength and failure mechanisms. Composites, Part B. 2016;94:197–208.
[42] Abed BH, Salih OS, Sowoud KM. Pinless friction stir spot welding of aluminium alloy with copper interlayer. Open Eng. 2020;10(1):804–13.
[43] Sharma A, Sharma VM, Gugaliya A, Rai P, Pal SK, Paul J. Friction stir lap welding of AA6061 aluminium alloy with a graphene interlayer. Mater Manuf Processes. 2020;35(3):258–69.
[44] Cao X, Shi Q, Liu D, Feng Z, Liu Q, Chen G. Fabrication of in situ carbon fiber/aluminum composites via friction stir processing: evaluation of microstructural, mechanical and tribological behaviors. Composites, Part B. 2018;139:97–105.
[45] Khidhir GI, Baban SA. Efficiency of dissimilar friction welded 1045 medium carbon steel and 316L austenitic stainless steel joints. J Mater Res Technol. 2019;8(2):1926–32.
[46] André NM, Goushegir SM, Santos J, Canto LB, Amancio-Filho ST, editors. On the microstructure and mechanical performance of Friction Spot Joining with additional film interlayer. Proceedings of the annual technical conference of society of plastics engineers (ANTEC 2014). USA: Society of Plastics Engineers; 2014.
[47] Campilho R, Pinto A, Banea MD, da Silva LF. Optimization study of hybrid spot-welded/bonded single-lap joints. Int. J Adhes Adhes. 2012;37:86–95.
[48] Nasir T, Kalaf O, Asmael M. Effect of rotational speed, and dwell time on the mechanical properties and microstructure of dissimilar AA5754 and AA7075-T651 aluminum sheet alloys by friction stir spot welding. Mater Sci. 2021. doi: 10.5755/j02.ms.26860.
[49] Asmael M, Glaissa M. Effects of rotation speed and dwell time on the mechanical properties and microstructure of dissimilar aluminum-titanium alloys by friction stir spot welding (FSSW). Materialwiss Werkstofftech. 2020;51(7):1002–8.
[50] André NM, Goushegir SM, dos Santos JF, Canto LB, Amancio-Filho ST. Influence of the interlayer film thickness on the mechanical performance of AA2024-T3/CF-PPS hybrid joints produced by friction spot joining. Weld Int. 2018;32(1):1–10.
[51] Devaraju A, Kumar A, Kotiveerachari B. Influence of addition of Grp/Al2O3p with SiCp on wear properties of aluminum alloy 6061-T6 hybrid composites via friction stir processing. Trans Nonferrous Met Soc. 2013;23(5):1275–80.
[52] Gao H, Huang Y. Geometrically necessary dislocation and size-dependent plasticity. Scr Mater. 2003;48(2):113–8.
[53] Shen Z, Yang X, Zhang Z, Cui L, Li T. Microstructure and failure mechanisms of refill friction stir spot welded 7075-T6 aluminum alloy joints. Mater Des. 2013;44:476–86.
[54] Amancio-Filho S, Bueno C, Dos Santos J, Huber N, Hage Jr E. On the feasibility of friction spot joining in magnesium/fiber-reinforced polymer composite hybrid structures. Mater Sci Eng A. 2011;528(10–11):3841–8.
[55] Esteves J, Goushegir S, Dos Santos J, Canto L, Hage Jr E, Amancio-Filho S. Friction spot joining of aluminum AA6181-T4 and carbon fiber-reinforced poly (phenylene sulfide): Effects of process parameters on the microstructure and mechanical strength. Mater Des. 2015;66:437–45.
[56] Khodabakhshi F, Haghshenas M, Sahraeinejad S, Chen J, Shalchi B, Li J, et al. Microstructure-property characterization of a friction-stir welded joint between AA5059 aluminum alloy and high density polyethylene. Mater Charact. 2014;98:73–82.
[57] Shorowordi KM, Haseeb A, Celis JP. Tribo-surface characteristics of Al–B4C and Al–SiC composites worn under different contact pressures. Wear. 2006;261(5–6):634–41.
[58] Arrabal R, Pardo A, Merino M, Mohedano M, Casajús P, Merino S. Al/SiC thermal spray coatings for corrosion protection of Mg–Al alloys in humid and saline environments. Surf Coat Technol. 2010;204(16–17):2767–74.
[59] Chandran P, Sirimuvva T, Nayan N, Shukla A, Murty SN, Pramod S, et al. Effect of carbon nanotube dispersion on mechanical properties of aluminum-silicon alloy matrix composites. J Mater Eng Perform. 2014;23(3):1028–37.
[60] Junaedi H, Abdo HS, Khalil KA, Almajid AA, editors. Aluminum–carbon metal matrix composites: effect of carbon fiber and aspect ratio on the mechanical properties. Adv. Mater. Res. 2015;1123:119–22.